Journal of Research High School

Vol. 2024 (11) 491 – 501
ISSN 2688-3651 [online]

Galactic Morphology Evolution of the SMACS 0723 Field Based on James Webb Space Telescope (JWST) Data Analysis

Franklin Yang[1] *

[1]Lynbrook High School, San Jose, CA, USA
*Corresponding Author: yang.franklin9@gmail.com

Advisor: Dr. David Taylor, David_taylor@fuhsd.org

Received July 18, 2024; Revised September 4, 2024; Accepted September 21, 2024

Abstract

The formation and evolution of galaxies are key processes that shaped the heterogeneous universe from a homogeneous state after the Big Bang. The advent of high-resolution space telescopes has provided unprecedented detail in observing distant and faint objects, enabling deeper analysis of galaxy morphology and structure that builds on the foundational classifications established by the Hubble Sequence. Aiming to study the galaxtic evolution in the Southern Massive Cluster Survey (SMACS) 0723 and identify the age of the more complex disk galaxies, this work examined the morphology of galaxies in using data from the James Webb Space Telescope (JWST). The captured high-resolution images provided new insights into galaxy formation and evolution, revealing a larger number of galaxies than previously visible with the Hubble Space Telescope. By applying the Morpheus machine learning model, 755 galaxies were identified and classified into four morphology categories: disk, spheroid, irregular, and point source. With more than 80% of the classified output receiving high confidence scores, this deep learning method was shown to be effective at analyzing JWST's high-resolution images, providing clearer and more detailed insights into galaxy morphology. The distributions of all types of galaxies throughout this cluster were found to be homogeneous, with the majority classified as disk galaxies. Additionally, by aligning JWST data with photometric redshift information from the Reionization Lensing Cluster Survey, this study presented a correlation between galaxy morphology and redshift; a substantial number of disk galaxies, over 50% of all galaxies, were identified at $z > 4$ for the first time. These findings suggest that disk galaxies have existed for billions of years, challenging previous assumptions about galaxy evolution. This research emphasizes the importance of JWST in advancing understanding of the universe and lays groundwork for future studies on galaxy morphology and evolution.

Keywords: Galactic evolution, Galactic morphology, James Webb Space Telescope, Redshift, Disk Galaxy

1. Introduction

The study of galaxy formation and evolution is concerned with the processes that formed the heterogeneous universe from a homogeneous beginning in the aftermath of the Big Bang (Benson, 2010). The formation of the first galaxies and their evolution over time directly determine the current universe. Launched into space in December 2021, The James Webb Space Telescope (JWST) orbits the Sun about 1 million miles from Earth. It is equipped with high-resolution and high-sensitivity instruments to view objects too distant or faint for its predecessors, such as the Spitzer Space Telescope and the Hubble Space Telescope (HST) (NASA, 2021).

The first publicly-released JWST image was a deep field image of the Southern Massive Cluster Survey (SMACS) 0723 (Dickmann, 2022). This massive cluster of galaxies is known to produce an extensive collection of gravitational arcs (Golubchik et al., 2022; Pascale et al., 2022). Finding a collection of red spiral galaxies that were not clearly

Vol. 2024 (11) 491 – 501
ISSN 2688-3651 [online]

present in the HST imaging, this research identified SMACS 0723 as an ideal resource for examining changes in galaxy morphology between HST and JWST imaging. In addition, the detailed morphological information provided by JWST would allow for more in-depth analysis of galaxy structure and evolution.

Playing a crucial role in determining its physical and dynamic properties, the morphology of a galaxy is most widely classified using the Hubble Sequence, also known as the Hubble Tuning Fork (Cavanagh, 2023; Conselice, 2014; Hubble, 1979). The Hubble sequence categorizes galaxies based on their morphology along a primary axi(Figure 1). At one end are spheroid galaxies with smooth, featureless light distributions and varying degree of llipticity, noted as E0 to E6. Spheroid galaxies are believed to form through cumulative merges over time (Hubble, 979; Martin et al., 2018). On the opposite end are spiral or disk galaxies, which are divided into two groups: those ith a central stellar bar, noted as SB0 to SBc, and those without, noted as S0 to Sc. They have flattened disk and aspiral structure, characteristic of star formation and galaxy collision (Graham et al., 2015). The most well-known example of a disk galaxy is the Milky Way where the Earth is located. Irregular galaxies, i.e., those with atypical shapes and often exhibit unique features, are included for completeness as an additional class beyond the spirals, noted as Irr in Figure 1. Spheroids are early-type galaxies, while disk galaxies are late-types, having evolved into more complex structures with time.

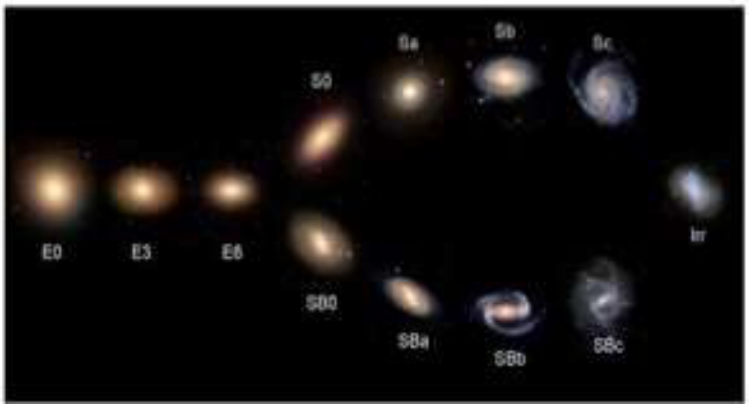

Figure 1. A depiction of the classification of galaxy morphologies using the Hubble Tuning Fork diagram (Cavanagh, 2023).

This work aimed at exploring the morphological evolution of the galaxies in the SMACS 0723 Field based on the latest data collected by JWST, whose scientific value goes far beyond visually stunning photographs. Given JWST's higher optical resolution and wider wavelength responsivity range, the it is hypothesized that previously unseen galaxies will be discovered in studied areas. For galaxies already observed in prior HST studies, it is also hypothesized that more detailed morphological information can be identified, leading to more precise morphology classification. The identification and classification of these newly discovered galaxies and re-classification of already identified galaxies according to the Hubble Sequence category is a labor-intensive task, especially for galaxies with transitional morphology. Classifying large numbers of galaxies requires not only expertise in galaxy morphology, but also efficiency in evaluation. Therefore, a major goal of this research aims to explore the morphological properties of the galaxies in the SMACS 0723 field through machine-learning (ML) based galaxy classification and measurement in an automated, accurate, and reliable way. JWST's near-infrared cameras (NIRCam) is used to investigate the morphology of early galaxies and uncover novel information inaccessible to HST, by assuming the galaxy morphologies in JWST images follow similar Hubble Sequence categorization and are suitable for ML models trained on previous telescope (e.g., HST) images. At the time of writing, there is no ML model that is specifically trained on JWST images and data; hence, an ML model trained based on HST and Spitzer Space Telescope images are used, with carefully examination the model's applicability to JWST by analyzing its classification confidence. Additionally, this work aims to study the age of the identified galaxies by redshift analysis. By leveraging the improved sensitivity to longer IR wavelengths from JSWT, correlating the galaxy morphology and age would provide important new details regarding aging in galaxy morphology evolution.

2. Materials and Methods

This work focused on analyzing the JWST images by processing data in three aspects: 1) morphology visualization in pseudo-color images, 2) pixel-level morphology classification with ML, and 3) galactic morphology

Vol. 2024 (11) 491 – 501
ISSN 2688-3651 [online]

evolution analysis via photometric redshift analysis.

Figure 2 shows the steps taken to process JWST and RELICS data using commercial software tools, custom software programs, and other analytical methods. The source data characterizing SMACS 0723 was part of the JWST Early Release Observations (EROs) taken on Aug 2, 2022, and was downloaded from the Mikulski Archive for Space Telescope (MAST) website (https://mast.stsci.edu/portal/Mashup/Clients/Mast/Portal.html). Among the many scientific instruments onboard JWST, this work used primarily the NIRCam in 7 bands (i.e., from 7 different narrow-pass filters): F090W, F115W, F150W, F220W, F277W, F356W and F444W. Designed to capture specific spectral information of a narrow wavelength band, these filters often correspond to the emission of specific elements such as hydrogen or helium. RELICS (Salmon et al., 2020) used for characterizing the redshift of galaxies was downloaded from a databased created by the Space Telescope Science Institute (STScI) and hosted on Amazon Web Service (AWS) (https://s3.amazonaws.com/grizli-v2/JwstMosaics/v7/smacs0723-grizli-v7.0-fix.photoz.tar.gz). For comparison between HST and JWST, HST data of SMACS 0723 was also downloaded from MAST, using the F105W, F606W, F140W, F814W, F160W, and F125W bands.

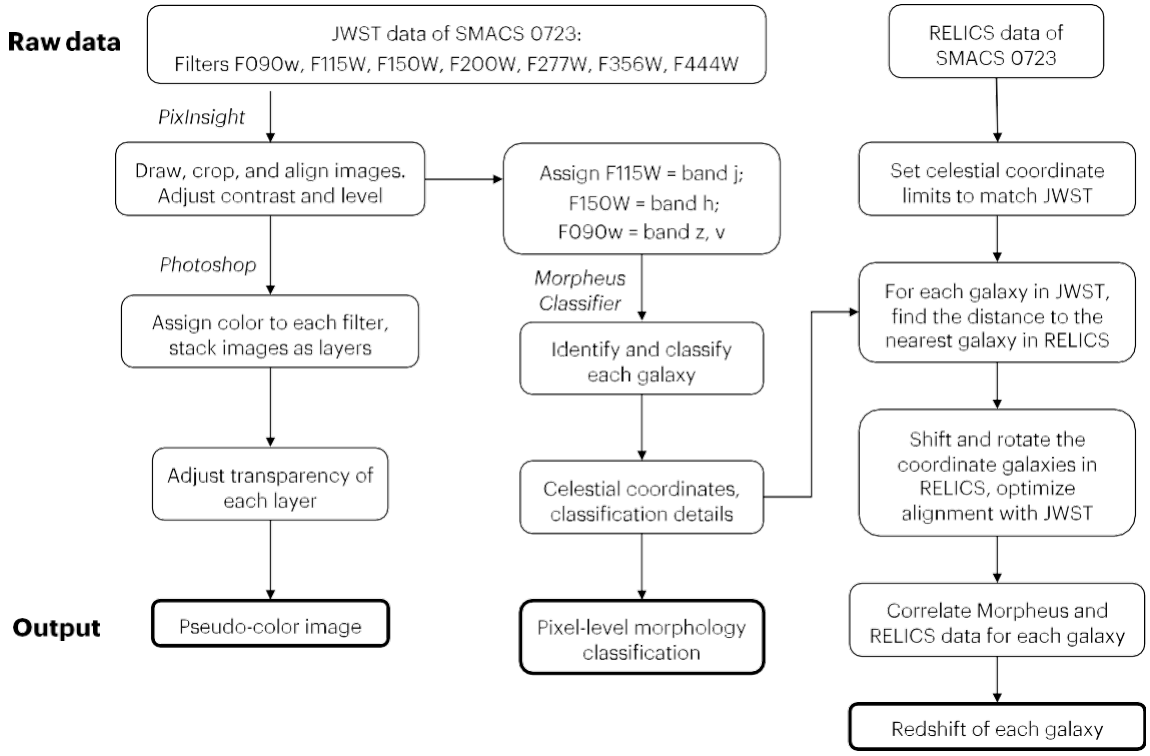

Figure 2. Data processing flow diagram. The two data sources (JWST and RELICS) were processed in multiple steps to generate three distinct analytical results: pseudo-color image, pixel-level morphology classification, and redshift of each galaxy.

2.1 SMACS 0723 galaxy morphology visualization

The high-resolution NIRCam images taken by JWST camera captures light invisible to human eyes. Thus, for visualization, it is necessary to synthesize a pseudo-color image by mixing multiple images, converting image data into visible colors following the rule of thumb of assigning purple and blue into relatively shorter-wavelength IR images and yellow and red to relatively longer-wavelength IR images. This work is summarized in Figure 3.

Raw image data files (.fits) of the 7 JWST NIRCam bands were downloaded from the MAST website and plotted as grayscale images using the commercial astrophysics software Pixinsight (Figure 3a). These images were aligned by rotating, shifting, and cropping borders such that galaxies identified with the Starfinder function of Pixinsight appear in the same locations on each image. Comparison of the 7 images showed that longer wavelength bands (e.g.,

Vol. 2024 (11) 491 – 501
ISSN 2688-3651 [online]

F444W with wavelength ~4.4 μm) captured more galaxies than shorter wavelength bands (e.g., F090W, F150W). This was already a positive indicator of the stronger galaxy detection capabilities of JWST compared to HST, where the longest-wavelength filter is only <1 μm. Following the JWST NIRCam coloring guideline (Figure 3b), each gray-scale image was tinted with a single color (Figure 3c), set to 50% transparency, and stacked as layers in Adobe Photoshop. Layers were mixed with the Screen Mode, and an overall brightness level adjustment of all layers was applied for optimal brightness and contrast. The final synthesized color image shown in Figure 3d reveals the high-resolution morphology and spatial distribution of galaxies in the SMACS 0723 cluster.

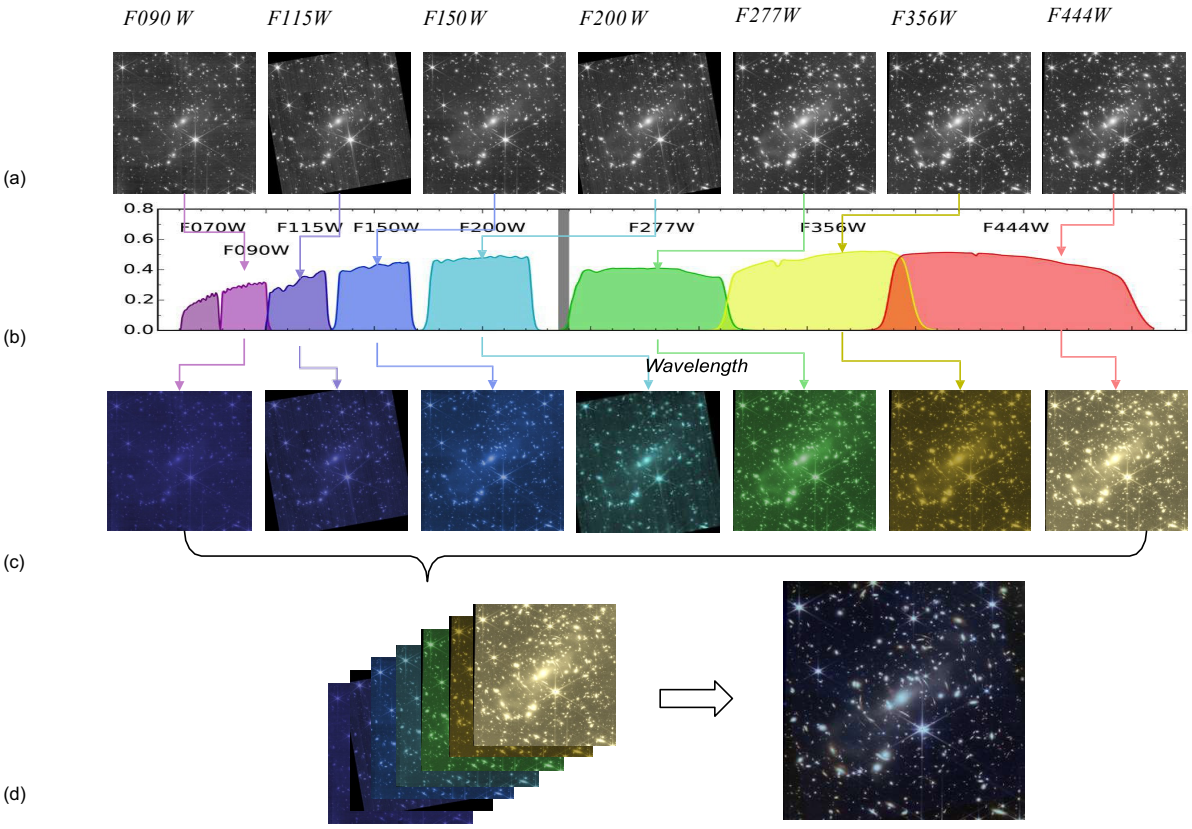

Figure 3. Pseudo-color image synthesis process and result. (a) Gray-scale images from JWST NIRCam raw data (.fits), each corresponding to a photo taken from a specific band, (b) JWST NIRCam coloring guidance provided by NASA (*JWST: Mid-Infrared Instrument (MIRI)*), (c) Each NIRCam image was tinted following the coloring guidance. (d) Each monochromatic image was set to 50% transparency and stacked as layers, leading to the final synthesized pseudo-color image.

2.2 ML-based galaxy morphology classification

Morpheus, an ML model developed by UC Santa Cruz in 2020, was used for simultaneous detection and morphological classification of astronomical objects through pixel-level semantic segmentation (Hausen & Robertson, 2020). Leveraging a deep learning neural network architecture following a U-Net configuration (Ronneberger et al., 2015), this model has proven that capable of simultaneous detection and morphological classification of astronomical objects through pixel-level semantic segmentation. It has successfully classified every pixel of the CANDELS survey into five morphological classes, demonstrating the ML model's accuracy and adaptability in astronomical morphology classification (Hausen & Robertson, 2020; Lanusse, 2023). Similar applications of U-Net can resolve other properties of galaxies, e.g., MAXIMASK (Paillassa et al., 2020); however, they are either limited to high-redshift galaxies (Huertas-Company et al., 2020), or focused on image artifacts only (Paillassa et al., 2020). In comparison, Morpheus

Vol. 2024 (11) 491 – 501
ISSN 2688-3651 [online]

has the suitable scope of surveying a large sky and classifying galaxies pixel by pixel. Additionally, the entire Morpheus library and demo project are open-source (https://github.com/morpheus-project/morpheus), allowing for easy understanding and adaptation to this work.

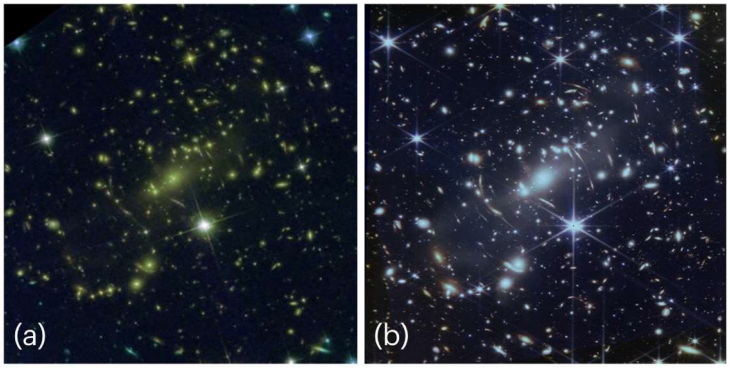

Figure 4. Color images of the SMACS 0723 field based on (a) HST data and (b) JWST data, synthesized in this work.

Approximately 1200 lines of codes were written in Jupyter Notebook (version 6.5.4) running python (version 3.11.3) to conduct multiple image processing and analysis tasks. This program was run on a Windows 11 computer with an AMD 5900X CPU and 32GB memory. These codes imported the Morpheus package, parsed the JWST data, ran neural network classification, analyzed model outputs, calculated statistics, and created images for visualization of results.

Since Morpheus was initially trained on Spitzer and HST images with their respective wavelengths, an effort was made in this work to ensure this training is applicable to JWST NIRCam images. Four images from different bands were provided to the Morpheus model, where filters with similar wavelength as the HST filters are used: F090W was used for band V, F090W for band Z, F115W for band J, and F150W for band H (Table 1). Since the shortest wavelength filter in JWST is F090W, it is used to represent both band V and band Z. These JWST filters were selected as they were close in wavelength to those from HST used in Morpheus training; this ensured the validity of the model on this new data. HST data was processed using a similar approach, where F606W was used for V, F850LP for Z, F125W for J, and F160W for W band images were used for Morpheus classification (Hausen & Robertson, 2020). Classification on full-size JWST images cropped to 4480 × 4523 pixels took 10.2 hours to process a total of 19913 batches.

Table 1. For each Photometric band, JWST Filters are selected as close proximity as the HST filters used for Morpheus training (Hausen & Robertson, 2020).

	HST Filters (STSCI, 2002)			JWST Filters (STSCI, 2024)		
Photometric Band	**Used in Morpheus training**	**Pivot λp (nm)**	**Width (nm)**	**Used in this work**	**Pivot λp (nm)**	**Width (nm)**
V	F606W	588.8	156.5	F090W	903	193
Z	F850LP	914.5	126.9	F090W	903	193
J	F125W	1248.6	284.5	F115W	1154	225
H	F160W	1536.9	268.3	F150W	1501	317

3. Results

3.1 JWST provides much improved morphology information

HST has revolutionized our understanding of the universe through its deep optical imaging of remote galaxies for over three decades and has provided some of the earliest detailed observations of galaxies in the distant universe (e.g., the Hubble Deep Field). HST's images have shown that galaxy morphology evolves over time, with distant galaxies appearing more irregular and compact compared to their closer, more mature counterparts. These findings have been crucial in mapping the history of galaxy formation and evolution, offering a clearer picture of the universe's early stage. Hence in this study, HST image is used as a baseline.

Aiming at the same SMACS 0723 cluster in the southern sky, the JWST color image synthesized in this work provided much higher resolution and clearer morphological details compared to the photo taken by HST in 2017 (Ronneberger et al., 2015), as shown in Figure 4. Table 2 gives the side-by-side comparisons of four example sections within the cluster and the classified galaxy types. The cutout sections of the HST, when zoomed in to the same level of those in the JWST, lack details that make it difficult to tell the morphology of the galaxy. The HST cutout section in the first two examples were so blurred that they were classified by the Morpheus ML model as background while

Vol. 2024 (11) 491 – 501
ISSN 2688-3651 [online]

the same cutout area was accurately classified as galaxies in the JWST image. Even at full zoomed-in, the synthesized JWST image shows clear details of each galaxy shape, spirals, and even distinguishes the existence of multiple galaxies in the last example. This is clear evidence that JWST image provides much more granular details of the morphology of individual galaxies, hence the morphology classification using the JWST data is more confident.

Table 2. Comparison of morphological details between HST and JWST. The image cutouts are portions from the full-size images in Figure 4.

HST Image Cutout		**JWST Image Cutout**	
Image	Morphology classification	Image	Morphology classification
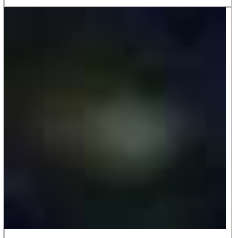	Background		Disk
	Background		Irregular
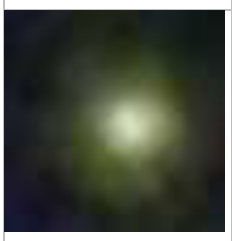	Spheroid		Spheroid
	Spheroid		2x Disk

3.2 Morphology classification results

The effectiveness of an ML classification is often measured by the confidence prediction from the model. In this work, the Morpheus classifier (Section 2.2) led to 81% of galaxy classifications having confidence scores above 0.7 (Figure 5a), and about half (49%) of the classifications score higher than 0.96. These results confirmed that the Morpheus classifier performed well on images taken by the JWST NIRCam. In other words, the galactic morphology categorization defined in the Hubble Sequence applied in the longer wavelength range up to 5.0 microns (i.e., band F444W).

The 408 identified galaxies were categorized as the following Hubble Sequence classifications: 3% spheroids, 11% irregular, and 85% disks. The distribution of these galaxy types in SMACS 0723 was mostly homogeneous.

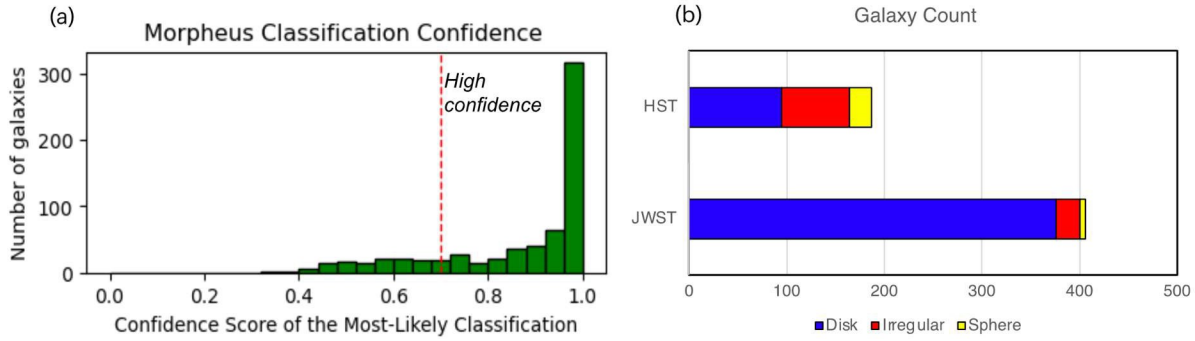

Figure 5. (a) Distribution of the Morpheus classification confidence of the 408 galaxies identified in the JWST image. (b) Count comparison of identified galaxies between JWST and HST images.

Vol. 2024 (11) 491 – 501
ISSN 2688-3651 [online]

These findings are significant, showing that the majority of galaxies in the SMACS 0723 cluster are disks with complex structures, matching visual morphology observation of the synthesized images (Figure 4, Table 2). Almost all of the 187 galaxies identified in the HST image were also found in the JWST image, and many additional galaxies were detected by JWST, bringing the total number of identified galaxies to 408. When grouped by galaxy type, both HST and JWST revealed that disk galaxies dominate this cluster, followed by irregular galaxies, while spherical galaxies are the least common in both images (Figure 5b).

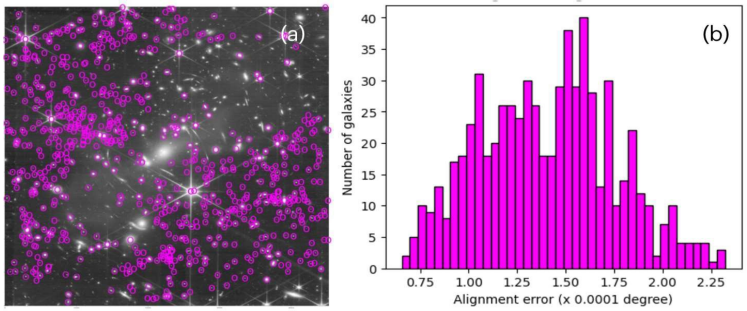

Figure 6. Alignment of galaxy coordinates between JWST and RELICS data. (a) Overlay of galaxy locations, with RELICES data on top of JWST image after minimizing alignment errors. Each purple circle marks the center of a galaxy in celestial coordinates (RA, Dec) from RELICS (Salmon et al., 2020). (b) Distribution of alignment error between JWST image and RELICS data.

3.3 Morphology evolution and redshift

The redshift of element emissions was used to characterize the age-related evolution of galactic morphology. This work aligned galaxy coordinates from JWST and RELICS (Salmon et al., 2020) to correlate morphological information from JWST with redshift information from RELICS for each identified galaxy.

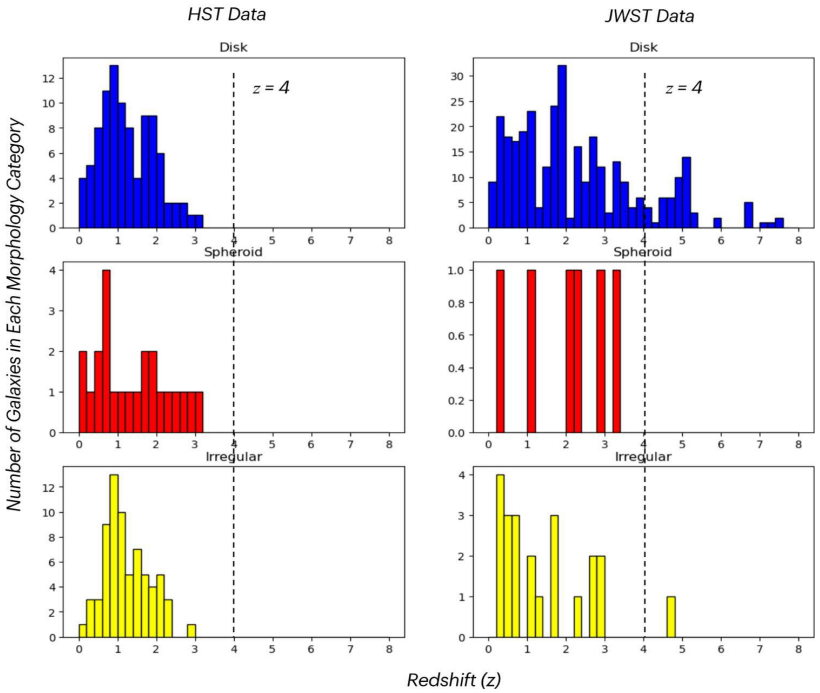

Figure 7. Distribution of identified galaxies in SMACS 0723 against their redshift (z) for each of the three galaxy types. The left column shows the result from HST data and the right column shows the result from JWST data.

A python script was developed to identify and match galaxies' location between JWST and RELICS data by translating, scaling, and rotating the two images formed from either data source to match each other (Figure 6). Using the celestial coordinates of RELICS data as the baseline, the SMACS 0723 cluster corresponded to the ranges of $110.8096736605 < RA < 110.8434963921$ and $-73.4816406633 < Dec < -73.4266137629$. Overlaying celestial coordinates of galactic centers from the RELICS on top of the JWST image showed a good alignment, as shown in Figure 6a. In addition, the distribution of the difference between galaxies' center coordinates from RELICS data and those calculated by Morpheus showed a good match, with an average alignment error of approximately 1.50×10^{-4} degrees (Figure 6b). This validation of alignment allowed for correlation between redshift measurement from RELICS and morphological analysis from JWST.

The morphologies of galaxies in SMACS 0723 were plotted against their redshift z-value. Each plot shows one of the three classes of galaxy types classified by the Morpheus ML model for data from HST and JWST, respectively

Vol. 2024 (11) 491 – 501
ISSN 2688-3651 [online]

(Figure 7). Redshifts of $z > 4.0$ require sensitivity in IR wavelengths > 4 μm, which is available for the first time via the JWST F444W filter. Unlike the HST observations that showed very few disk galaxies at $z > 2$ and a rapid decrease at higher redshifts (left column in Figure 7) which confirms observations from (Huertas-Company et al., 2016; Mortlock et al., 2013), this new galaxy distribution observed from JWST data shows a large number of disk galaxies at $z > 2$, and a significant number of galaxies even have $z > 4$. In contrast, only 5 spheroid galaxies are identified by Morpheus from this new data, and all with a small redshift of $z < 4.0$. Additionally, the number of disk galaxies are much larger than that of Irregular galaxies, showing significantly less distortion than previously believed (Mortlock et al., 2013). Larger z-values correspond to older galaxies, showing that disk galaxies in this cluster have existed in large quantities for a significant amount of time. This result is interesting, implying that disk galaxies such as the Milky Way could have had the same complex disk morphology for over 12 billion years, similar to the disk galaxies in SMACS 0723. Although contrary to the conventional wisdom, this finding is supported by independent research using different morphology classification software, tweakreg (part of DrizzlePac) and astropy reproject, which drew a similar conclusion that disk galaxies have existed for over 10 billion years (Ferreira et al., 2022). Using JWST analysis, another work also found that thin disk galaxies formed as early as <1 billion years from the Big Bang (Nepal et al., 2024), matching the 12 billion year age estimate of the early disk galaxies found in this work.

It is noted that among the 23 spheroid galaxies identified in the HST image, only 6 are confirmed in the JWST age (Figure 5b). These spheroids are randomly and homogeneously distributed in SMACS 0723, while noticeably all smaller compared to their disk and irregular neighbors (Figure 8). The reduced number of spheroids can be attributed to the increased resolution in JWST leading to re-classification as other types. Most of the early-formed spheroids have likely already evolved into more complex disk or irregular types; these 6 spheroids were likely created during a collision or merger, thus having younger ages as shown by the z < 4 redshift (Figure 7).

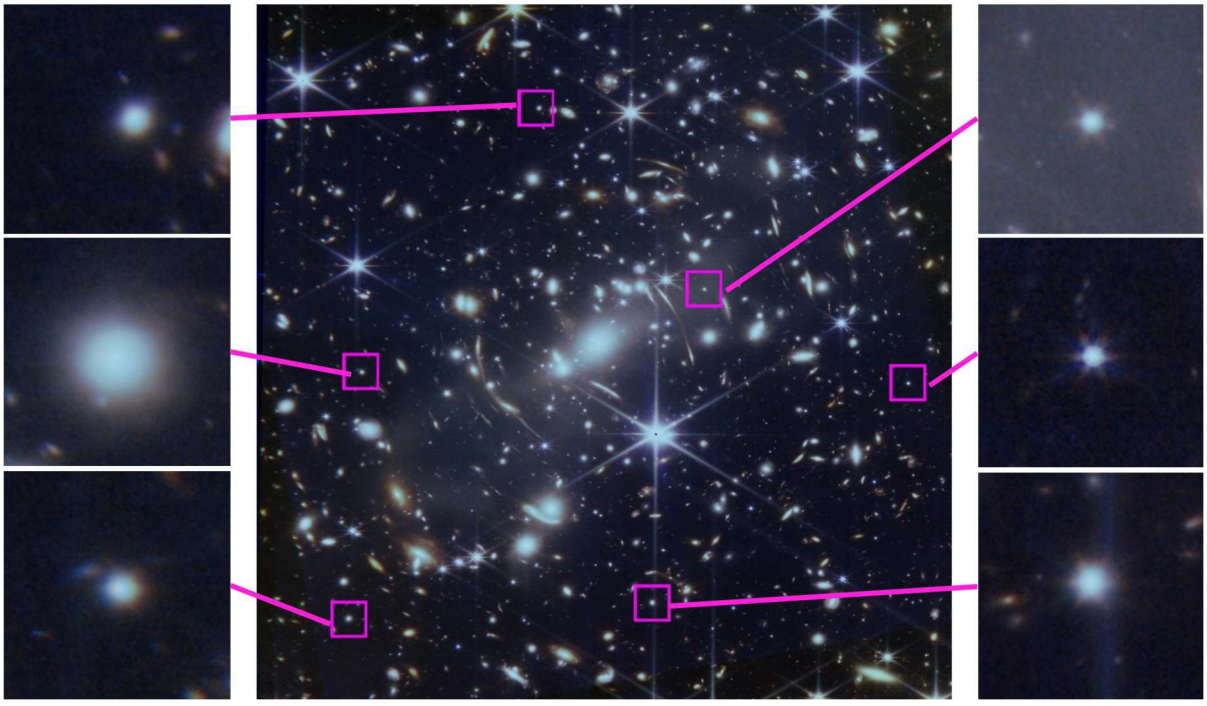

Figure 8. Six spheroid galaxies are identified in SMACS 0723.

3.4 Age and the Hubble Sequence

The Hubble Sequence is a classification scheme that outlines the morphological evolution of galaxies, so a natural question arises: when did the first complete Hubble Sequence emerge? It is well established that the earliest galaxies, formed shortly after the Big Bang, were simple spherical galaxies. These early galaxies lacked the complex structures

Vol. 2024 (11) 491 – 501
ISSN 2688-3651 [online]

seen in later formations. Over time, more intricate disk galaxies developed, a process evidenced by the observation that most disk galaxies are found at $z < 4$. However, the findings from this study reveal the existence of disk galaxies at higher redshifts, extending beyond $z > 4$, plus an irregular galaxy identified at $z = 4.7$. This suggests that elements of the Hubble Sequence, including more advanced morphological types, are present at redshifts of $z > 5$. Consequently, the full morphological evolution of the Hubble Sequence, including the formation of both elliptical and disk galaxies, likely occurred at least 10 billion years ago, indicating an earlier establishment of galactic diversity than the previous estimation of $z \sim 2$ (Conselice, 2004).

4. Discussion

In this work, the main discovery using JWST data is the existence of a large number of disk galaxies at high redshift than originally believed, which implies that disk galaxies have formed and existed for a significant amount of time, up to several billions of years. They are additionally found to be much more common than originally thought, thus raising the question of how often these galaxies are formed through merges (Duncan et al., 2019). In addition, this study shows that the number of disk galaxies is significantly fewer than that of spheroids, suggesting the possibility that SMACS 0723 field may have evolved to a mature state where the generation of new galaxies has slowed down.

The analytical method used in this work can be extended to other JWST images. With the continued public release of additional JWST observational data, more galaxies can be identified, and their morphology classified following the approach described in this work. Future studies may also examine non-cluster regions and larger areas for more comprehensive analyses. Further analysis could explore the formation of spheroids and disk galaxies at high redshifts, and the role of mergers in galaxy evolution. Detailed examination of resolved structures in galaxies can help in understanding the process of disk formation at high redshifts. Additionally, future studies could investigate the relationship between galaxy morphology and physical properties. JWST's NIRCam and MIRI data could be used to probe the relationship between the morphology and stellar mass at $z > 3$, for instance, by analyzing the morphology of a selected sample of star-forming and quiescent galaxies, focusing on parameters like effective radius, Sérsic index, and axis ratio (Gómez-Guijarro et al., 2023; Ito et al., 2024). These morphological features may be correlated with stellar mass to identify trends and differences between galaxy types. By comparing galaxies across different redshifts, it may be possible to uncover evolutionary trends that enhance understanding of the physical processes driving galaxy growth and transformation over time.

5. Conclusion

With over three decades of data, HST continues to be an active and invaluable resource for understanding the universe. Though operating on slightly different wavelength ranges, many astrophysics tools and methods developed using HST data can be adapted and validated for use with data from the JWST due to a large shared wavelength range. This study utilized JWST data to analyze the morphology of galaxies at high redshifts using the Morpheus deep learning framework for pixel-level astronomical morphology classification and demonstrated that the morphology classification means embedded in Morpheus can be successfully applied to JWST data without issues. JWST provided clearer and more detailed images compared to previous technologies, allowing for a better understanding of galaxy morphology and structure. The Morpheus model identified and classified 755 galaxies in deep space SMACS 0723, significantly more than previously found. This result demonstrated that the Morpheus deep learning model could drastically speed up morphology analysis of JWST observations and accelerate the discovery of new galaxies. The Hubble Sequence was found to be established at high z-values, with a significant number of disk galaxies identified at $z > 4$, implying disk galaxies have existed in large numbers for tens of billions of years. Supported by other research (Ferreira et al., 2022; Nepal et al., 2024), these findings challenge previous assumptions about galaxy evolution and highlight the importance of JWST in advancing understanding of galaxy formation and evolution.

Acknowledgments

The author is indebted to Mr. David Taylor for his indispensable support in this work.

Vol. 2024 (11) 491 – 501
ISSN 2688-3651 [online]

References

Benson, A. J. (2010). Galaxy formation theory. *Physics Reports*, *495*(2-3), 33-86. Cavanagh, M. (2023). Morphological evolution of galaxies with deep learning.

Conselice, C. J. (2004). The Formation of the Hubble sequence. Multiwavelength Cosmology: Proceedings of the "Multiwavelength Cosmology" Conference, held on Mykonos Island, Greece, 17–20 June, 2003,

Conselice, C. J. (2014). The evolution of galaxy structure over cosmic time. *Annual Review of Astronomy and Astrophysics*, *52*, 291-337.

Dickmann, N. (2022). *Amazing Night Sky Atlas*. Lonely Planet.

Duncan, K., et al. (2019). Observational Constraints on the Merger History of Galaxies since z ≈ 6: Probabilistic Galaxy Pair Counts in the CANDELS Fields. *The Astrophysical Journal*, *876*(2), 110. https://doi.org/10.3847/1538-4357/ab148a

Ferreira, L., et al. (2022). Panic! at the Disks: First Rest-frame Optical Observations of Galaxy Structure at z> 3 with JWST in the SMACS 0723 Field. *The Astrophysical Journal Letters*, *938*(1), L2.

Golubchik, M., et al. (2022). HST Strong-lensing Model for the First JWST Galaxy Cluster SMACS J0723. 3− 7327. *The Astrophysical Journal*, *938*(1), 14.

Gómez-Guijarro, C., et al. (2023). JWST CEERS probes the role of stellar mass and morphology in obscuring galaxies. *Astronomy & Astrophysics*, *677*, A34.

Graham, A. W., et al. (2015). Hiding in Plain Sight: An Abundance of Compact Massive Spheroids in the Local Universe. *The Astrophysical Journal*, *804*, 32. https://doi.org/10.1088/0004-637x/804/1/32

Hausen, R., & Robertson, B. E. (2020). Morpheus: A Deep Learning Framework for the Pixel-level Analysis of Astronomical Image Data. *The Astrophysical Journal Supplement Series*, *248*(1), 20. https://doi.org/10.3847/1538-4365/ab8868

Hubble, E. P. (1979). Extra-galactic nebulae. In *A Source Book in Astronomy and Astrophysics, 1900–1975* (pp. 716-724). Harvard University Press.

Huertas-Company, M., et al. (2016). Mass assembly and morphological transformations since z ∼ 3 from CANDELS. *Monthly Notices of the Royal Astronomical Society*, *462*, 4495-4516. https://doi.org/10.1093/mnras/stw1866

Huertas-Company, M., et al. (2020). Stellar masses of giant clumps in CANDELS and simulated galaxies using machine learning. *Monthly Notices of the Royal Astronomical Society*, *499*(1), 814-835.

Ito, K., et al. (2024). Size–Stellar Mass Relation and Morphology of Quiescent Galaxies at z≥ 3 in Public JWST Fields. *The Astrophysical Journal*, *964*(2), 192.

JWST: Mid-Infrared Instrument (MIRI). NASA. Retrieved Sep 20, 2022 from https://jwst.nasa.gov/content/observatory/instruments/miri.html

Lanusse, F. (2023). The Dawes Review 10: The impact of deep learning for the analysis of galaxy surveys. *Publications of the Astronomical Society of Australia*, *40*, e001.

Martin, G., et al. (2018). The role of mergers in driving morphological transformation over cosmic time. *Monthly Notices of the Royal Astronomical Society*, *480*(2), 2266-2283. https://doi.org/10.1093/mnras/sty1936

Vol. 2024 (11) 491 – 501
ISSN 2688-3651 [online]

Mortlock, A., et al. (2013). The redshift and mass dependence on the formation of the Hubble sequence at z > 1 from CANDELS/UDS. *Monthly Notices of the Royal Astronomical Society*, *433*, 1185-1201. https://doi.org/10.1093/mnras/stt793

NASA. (2021). *Webb Space Telescope*. Retrieved February 25, 2024 from https://www.jwst.nasa.gov/index.html

Nepal, S., et al. (2024). Discovery of the local counterpart of disc galaxies at z> 4: The oldest thin disc of Milky Way using Gaia-RVS. *arXiv preprint arXiv:2402.00561*.

Paillassa, M., et al. (2020). MAXIMASK and MAXITRACK: Two new tools for identifying contaminants in astronomical images using convolutional neural networks. *Astronomy & Astrophysics*, *634*, A48. (n)

Pascale, M., et al. (2022). Unscrambling the Lensed Galaxies in JWST Images behind SMACS 0723. *The Astrophysical Journal Letters*, *938*(1), L6.

Ronneberger, O., et al. (2015). U-Net: Convolutional Networks for Biomedical Image Segmentation. In N. Navab, J. Hornegger, W. M. Wells, & A. F. Frangi, *Medical Image Computing and Computer-Assisted Intervention – MICCAI 2015* Cham.

Salmon, B., et al. (2020). RELICS: The Reionization Lensing Cluster Survey and the Brightest High-z Galaxies. *The Astrophysical Journal*, *889*(2), 189. https://doi.org/10.3847/1538-4357/ab5a8b

STSCI. (2002). *Hubble Space Telescope User Documentation, IR Spectral Elements*. https://hst-docs.stsci.edu/wfc3ihb/chapter-7-ir-imaging-with-wfc3/7-5-ir-spectral-elements

STSCI. (2024). *JWST User Documentation, NIRCam Filters*. https://jwst-docs.stsci.edu/jwst-near-infrared-camera/nircam-instrumentation/nircam-filters#gsc.tab=0